Mesoscale Convective System Rainfall in the Sahel

VINCENT MATHON, HENRI LAURENT, AND THIERRY LEBEL

LTHE, IRD, Grenoble, France

(Manuscript received 15 June 2001, in final form 20 May 2002)

ABSTRACT

Based on a full-resolution Meteosat dataset, an extensive climatological study of the mesoscale convective systems (MCSs) observed by satellite over the Sahel leads to the definition of a subpopulation of MCSs—called organized convective systems (OCSs)—that represents only 12% of the total number of MCSs observed during 9 yr over the central Sahel while accounting for almost 80% of the total convective cloud cover defined at the 233-K threshold. Using a high-resolution rainfall dataset, it is shown that these OCSs are also the main source of rain in this region, accounting for about 90% of the seasonal rainfall, with a mean areal rainfall of 14.7 mm per system. All of the OCSs are associated with a rain event, and more than 90% of the major rain events are associated with an OCS. These figures are compared with those obtained for mesoscale convective complexes (MCCs). Each MCC produces more rainfall on average (19 mm per system) but there are only a few of them (1.2% of the total number of MCSs), and they consequently produce only 19% of the seasonal rainfall. The interannual rainfall variability is first determined by the year-to-year fluctuation of the number of events defined from satellite rather than by the fluctuations of their mean rain efficiency. In fact, the total rain yield of an OCS appears to be linked primarily to its duration (which itself is largely determined by its spatial extension) rather than to its average rain rate. The diurnal cycle over the region is also studied, and it is shown that it is largely conditioned by the propagative nature of the OCSs associated with orography-driven generations located a few hundred kilometers to the east of the validation area.

1. Introduction

Tropical convective clouds often evolve into organized clusters with anvils merging into a single mesoscale cloud shield (Houze 1993). This configuration is commonly referred to as a mesoscale convective system (MCS). Since the end of the 1970s, geostationary satellite data have made possible a precise identification and tracking of MCSs. Because of the availability of large datasets of infrared images, several studies were conducted in the 1980s and 1990s to characterize the life cycle of large MCSs in various regions of the world.

In his pioneering work, Maddox (1980) was the first to define a subset of large and well-organized MCSs, widely known since as mesoscale convective complexes (MCCs). Many ensuing studies have focused on the MCCs because they are only few in number but account for a significant share of cloud coverage (e.g., Miller and Fritsch 1991; Laing and Fritsch 1993).

Even though it has long been recognized that tropical convective clouds account for most of the tropical precipitation (e.g., Houze 1981), there are relatively few studies that are aimed at a precise estimation of the rainfall associated with either MCSs or MCCs in the tropical regions. In recent studies carried out over Africa, Laing et al. (1999) estimated that 22% of Sahelian rainfall was produced by MCCs, whereas Mathon and Laurent (2001), using a different definition, estimated that MCCs contribute only about 15% of the convective cloud cover. Laurent et al. (1997) previously found that, over the region of Niamey, Niger, most of the intense rain events producing 80% of the annual rainfall were associated with large cloud clusters easily identified from infrared imagery.

The various studies cited above illustrate the need to define as precisely and objectively as possible what a rain-efficient MCS is in the Sahel and which subpopulation of MCS should be monitored to account for the largest possible share of the total rainfall. This paper therefore intends to provide reliable statistics on the rainfall associated with the Sahelian MCSs based on the combination of two datasets covering 9 yr (1990–94 and 1996–99): a high-resolution satellite imagery database and the Etudes des Précipitations par Satellite (EPSAT)-Niger (EN) ground rainfall dataset (Lebel et al. 1992). The central issue of this paper, discussed in section 2, is to define as objectively as possible a population of rain events from in situ observations and a subpopulation of rain-efficient convective systems from satellite imagery. Sections 3 and 4 describe how these definitions are applied to the EN dataset and to the Meteosat dataset, respectively. In section 5, a climatological description of rainfall from Sahelian MCSs is given, based on statistics computed for two different subpopulations of MCSs. Section 6 focuses on analyzing some

Corresponding author address: Thierry Lebel, LTHE, BP 53, 38041 Grenoble Cedex 9, France.
E-mail: thierry.lebel@inpg.fr

TABLE 1. Criteria commonly used to define populations of rain events and convective systems.

	Rain events	Convective systems
Sensor	Recording rain gauges	Satellite radiometers
Data	Accumulated rain depth	IR brightness temperature
Intensity (magnitude) criterion	Min rain depth at one or several gauges	Threshold temperature
Space (size) criterion	Proportion of rain gauges recording rain	Continuous area above threshold temperature
Time criterion	Min duration with no rainfall between two consecutive events	Min life duration of the cluster

aspects of the interannual variability of these statistics. A final section is devoted to the discussion of the results presented in sections 5 and 6.

2. Mesoscale convective systems and rain events

A rainfall regime may be crudely defined by the average occurrence rate of rain events and by the average magnitude of these events. These two parameters vary from region to region and, within a region, display a seasonal cycle. Detecting whether one, or both, parameters are changing—and in what sense—during dry years may provide clues regarding the atmospheric causes of droughts in the Sahel. However, defining a rain event is not straightforward. Indeed, the definition is conditioned by the sensor or combination of sensors used. On the one hand, cloud clusters are observed well from a geostationary satellite, but not all of these clusters are producing significant rain. Imposing thresholds in temperature, duration, and size is the common way to select the supposedly most efficient cloud clusters in terms of rainfall. On the other hand, it is possible to define directly from a rain gauge network a sample of important rain events. This approach leads to defining rain events as space–time ground rain structures. However, the characteristics of the population so defined are network dependent; that is, they may change with the spatial coverage of the network and with the sampling properties of the gauges. Given this, obtaining two coincidental populations of cloud clusters and rain events is not easy. It may be seen from Table 1 that the criteria used to define these two entities are both similar and distinct. One major reason for this is the difference in nature of the sensors used for identifying cloud systems or rain events. Infrared satellite images provide a global view of the convective systems but their rainfall quantification is very inaccurate. Rain gauge networks give precise quantitative information but at given points only, and the identification of rain events requires ad hoc hypotheses and specific algorithms.

In the Sahel, where operational ground networks are sparse and composed of daily reading gauges only, the EN dataset is the only one to cover several years and to allow for a precise identification of rain events. Combined with full-resolution geostationary satellite images, the EN observations thus provide a unique opportunity to establish a climatological rainfall description of the Sahelian MCSs.

3. Rain-event climatological description in the Sahel

a. Dataset

To produce a consistent climatological description, including interannual variability, it is necessary to use rainfall observations sampled at a time interval smaller than one day because the typical duration of a rain event in the Sahel is on the order of a few hours. One motivation of the EPSAT-Niger experiment (Lebel et al. 1992) was precisely to provide such observations that are lacking in operational networks, which report daily readings of rain. The experiment started in 1990 with 100 recording rain gauges (minimum recording threshold of 0.5 mm) covering a 160×110 km^2 area, hereinafter referred to as the EN area (Fig. 1). In 1994, the network was reduced to 30 gauges. Lebel and Amani (1999) have shown that such a network was able to estimate accurately the average rainfall over the EN area from the event level to seasonal scales and beyond. The data used in this work are event rainfall accumulations obtained at each station from the original series of 5-min rainfall recorded by the 30-gauge network over 1990–94 and 1996–99.

b. EPSAT-Niger rain events

The criteria listed in Table 1 to define a rain event from rain gauge measurements can be computed either for a single gauge or for an ensemble of gauges. When using a single gauge, there is great sensitivity to the time parameter used to separate two consecutive events. In this respect, one important advantage of the EN network is the ability to use an ensemble of gauges to define a rainfall event. Because the area covered by the network and the area covered by an MCS are of comparable size, the probability of observing two different systems at the same time over the EN area is relatively low. Therefore, it was decided to define a rain event in the following way:

1) At least 30% of the gauges (ground space criterion: α_g) must record an event rain depth equal to or greater than 1 mm (ground intensity criterion: i_g).
2) There should not be a rainfall interruption of more than 30 min (ground time criterion: τ_g) over the whole network. If all gauges do not report any rain during a continuous 30-min period, then it is the end of the rain event.

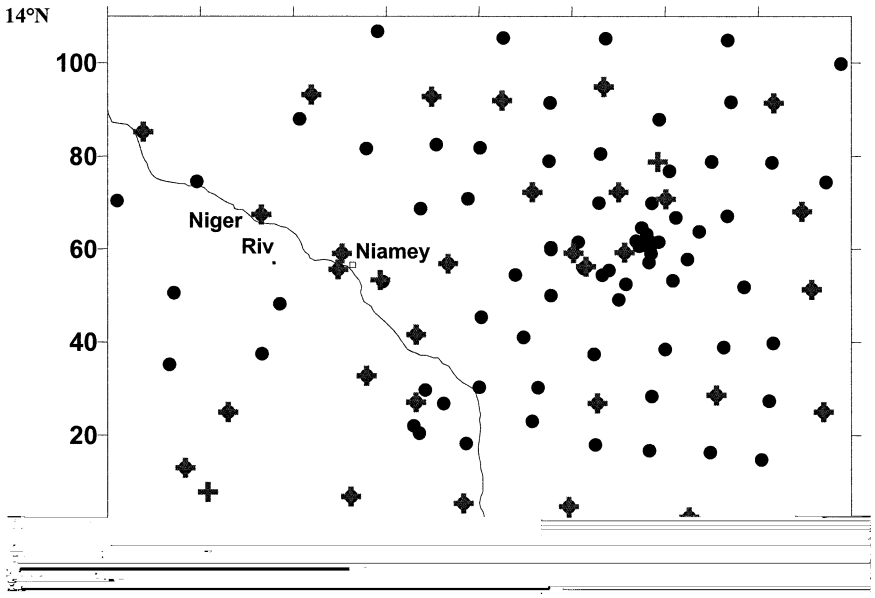

FIG. 1. The EN recording network. Coordinates are in kilometers with the origin at 13°N, 2°E. Black circles are the stations of the dense network in operation from 1990 to 1993. Crosses are the stations of the long-term monitoring network in operation from 1990 to 1999.

An extensive study of the sensitivity of the number of events to the value of τ_g and i_g showed some stability around the values chosen above. In fact, reducing τ_g to 15 min or increasing i_g to 2 mm produces only minor variations in the number of events (on the order of 1%–2%).

With these criteria (i.e., $\alpha_g = 30\%$, $i_g = 1$ mm, and $\tau_g = 30$ min), the total number of rain events observed over the EN area in 9 yr is 387, with an average rain depth per event of 10.2 mm. The average proportion of gauges recording no rainfall during an EN rain event is 26%, so the average point rain depth, conditional to rain being observed at a station, is 13.8 mm.

c. Rain-event classification

D'Amato and Lebel (1998) proposed a simple classification of the EN rain events based on the proportion of gauges recording rainfall ($\alpha_g > 30\%$). They also showed that rain events with at least 80% of the gauges recording rainfall ($\alpha_g > 80\%$) explain more than 70% of the total rainfall while accounting for approximately 50% of the total number of rain events. Henceforth, rain events satisfying the ground space criterion $\alpha_g > 80\%$ are called "major rain events." For the 9 yr covered by this study, a total of 253 rain events were recorded by the EN network during the core of the rainy season (1 July–15 September), 144 of which are major rain events. Table 2 shows that 72% of the rain (or 361 out of 499 mm) falls during the core of the rainy season. This proportion has decreased in recent years. In the 1950s and 1960s, the mean annual rainfall in the Niamey area was about 650 mm, with about 510 mm falling during the period 1 July–15 September, that is, about 78%. From Table 2 it is also seen that both the EN events and the EN major events account for a slightly larger share of rain during the core of the rainy season (91% and 73%, respectively, against 88% and 70%, respectively, over the whole rainy season).

TABLE 2. Rainfall statistics over the EN area. The statistics are computed for 1990–99 (1995 excluded) for the whole rainy season in the first line and for the core of the rainy season (1 Jul–15 Sep) in the second line.

	Total (mm)	EN rain events (mm)	Major EN rain events (mm)
Annual rainfall	499	439 (88%)	349 (70%)
1 Jul–15 Sep	361	328 (91%)	263 (73%)

4. MCS identification from satellite imagery

a. MCS tracking

Ten years (1990–99) of full-resolution (30 min; 5×5 km^2) Meteosat infrared channel (10.5–12.5 μm) images covering the 1 July–15 September period were archived for this study. However, 1995 is not used because 10 days of data are lacking in July. The statistics presented here were thus computed over a period of 9 yr: 1990–94 and 1996–99. Over this period the proportion of time with no data is 8%. From year to year, this proportion fluctuates between 1% and 14% (Table 3). As explained below, the final proportion of time with no tracking was significantly reduced by a linear interpolation scheme.

MCS identification was carried out through a tracking algorithm based on an areal overlap method, similar to

TABLE 3. Fraction of total missing images and fraction of missing images that cannot be interpolated (gaps larger than five consecutive hours).

Year	Missing images (%)	Gaps > 5 h (%)
1990	8	5
1991	7	5
1992	6	0
1993	13	0
1994	14	0
1996	12	2.5
1997	12	0
1998	1	0
1999	2	0

those described by Williams and Houze (1987). The method and the quality of the results it produces are discussed in detail in Mathon and Laurent (2001). Thus, only its main features are recalled below.

Convective clouds are delineated in Meteosat infrared images using two different brightness temperature thresholds: 233 and 213 K. The 233-K threshold is in the range of the most commonly used thresholds for identifying deep convection (Duvel 1989) and accumulated convective precipitation in the Tropics (Arkin 1979). The 213-K threshold targets the most active part of the convective systems. Moreover, the 213-K threshold was found by some authors as an optimum for correlating cloud occurrences and rainfall during the core of the rainy season over the central Sahel (Jobard and Desbois 1992).

The tracking method is only applied to convective clouds larger than 5000 km^2. Below this value, tracking is difficult to implement because the cloud number increases strongly, whereas the overlapping surface tends to be limited. Mathon and Laurent (2001) have shown that, despite the 5000-km^2 size cutoff, the cloud life cycles obtained are very close to what could be produced by a manual method. Moreover, they calculated that only 7% (9%) of the total cloud cover at the 233-K (213 K) threshold are lost because of the filtering of small clouds.

The effect of missing data on the tracking results is limited by using an interpolation scheme. It basically consists of generating virtual images and running the tracking process as if there were no missing images. These virtual images are generated by extrapolating the displacement of each cloud present in the last actual image. It has been shown that this interpolation scheme generates cloud occurrences very close to the actual ones, and that this process is of particular interest to estimate the actual number of convective clouds (Mathon and Laurent 2001). However, when more than 10 successive images are missing, the tracking is not carried out. Table 3 gives the fraction of missing images for each year. There were only a few cases in 1990, 1991, and 1996 when the interval of missing images was larger than 5 h. The interpolation scheme allows reduction of the proportion of missing hours over the whole period of study from 8% to 1.4%.

Mesoscale convective systems are defined as convective clouds larger than 5000 km^2 at the 233-K threshold. There are several reasons for the choice of this temperature threshold:

- The 233-K threshold is in the range of the most common thresholds used to define MCS (Machado et al. 1992, 1998) and MCS subpopulations, such as MCCs (Laing and Fritsch 1993) or squall lines (Rowell and Milford 1993).
- As already mentioned, 233 K is in the range of the temperature thresholds used in satellite-derived rainfall estimation algorithms (Arkin 1979).

MCSs as defined above contribute to 93% of the total Sahelian cloud coverage at the 233-K threshold for the core of the Sahelian rainy season (1 July–15 September).

b. Classification of the Sahelian mesoscale convective systems

At the early stage of MCS studies from satellites it was found that very deep convection associated with the heaviest rainfall was most likely to be found in large MCSs displaying some specific structure. Such systems are noticeably characterized by large trailing anvils and by the presence of intense convective cells imbedded in mesoscale clusters. Maddox (1980) was the first to define numerical criteria allowing for an objective identification of a particular set of such systems that were called MCCs. In the Sahel, however, MCCs account for a small fraction of either rainfall or cloud cover, as mentioned in section 1. There is thus a need to identify a larger subsample of MCSs so as to include most of the rain-producing systems.

Based on the radar data acquired during field experiments, such as the Global Atmospheric Research Program (GARP) Atlantic Tropical Experiment (GATE) and the Convection Profonde Tropicale (COPT) experiment (e.g., Zipser 1977; Houze 1977; Roux 1988), Houze (1981) divided the tropical cloud clusters into squall and nonsquall clusters. First described by Hamilton and Archbold (1945) for West Africa, squall lines produce heavy rainfall and are characterized by a unique and well-defined structure, documented in radar data and simulated in numerical studies (e.g., Redelsperger and Lafore 1988; Lafore and Moncrieff 1989). Squall lines are likely to contribute to a large share of the Sahelian precipitation, but it is not easy to find objective criteria to identify them in a population of MCSs. In their studies over West Africa, Desbois et al. (1988) and Rowell and Milford (1993) used a sharp-leading-edge criterion. However, cases of MCSs that do not present a well-defined leading edge on satellite images may prove to present a typical squall line structure on radar images, as shown by Smull and Houze (1985) and by Lebel et al. (1997).

The most obvious way to establish a comprehensive

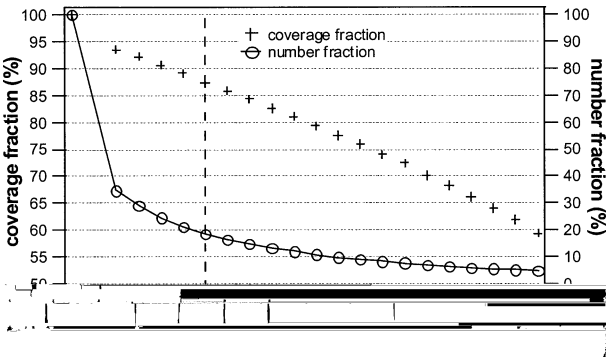

FIG. 2. The 233-K MCS coverage fraction (crosses) and number fraction (line and circles) vs lifetime of the 213-K clusters embedded in the 233-K MCS cloud shield. The first selection criterion is indicated as a vertical line at lifetime = 3 h.

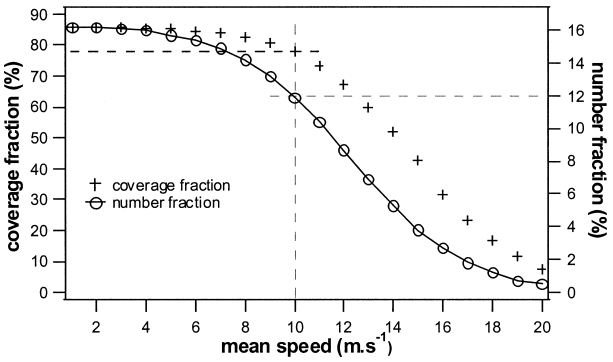

FIG. 3. The 233-K MCS coverage fraction (crosses) and number fraction (line and circles) vs mean speed of the embedded 213-K clusters. Only MCSs passing the first selection criterion have been considered here. The second criterion is indicated as a vertical line at speed = 10 m s^{-1}.

climatological description of rainfall from satellite data is to relax the criteria commonly used to define MCCs. The selection proposed here is based on two temperature thresholds: 233 and 213 K. When studying the life cycle of 213-K clusters (i.e., continuous 213-K areas larger than 5000 km^2), it appears that using two numerical criteria allows us to select a small number of MCSs associated with a large proportion of the total cloud cover at 233 K. The first criterion is related to the lifetime of the 213-K clusters. Figure 2 shows the number fraction and coverage fraction of the 233-K MCSs as a function of the lifetime of their 213-K clusters. The first class (0 h) corresponds to 233-K MCSs, which do not contain any cluster at 213 K tracked by the algorithm. Note that most systems are located in this first class. The two distributions appear markedly different, which shows that a small number of systems account for most of the total cloud coverage. The 3-h threshold was chosen as a compromise to select potentially rain-efficient MCSs. Systems with a 213-K cluster lasting for more than 3 h are 18% in number but account for 87% of the total 233-K cloud coverage.

In a second step, the selection is refined by using a mean speed criterion. Houze (1981) states that squall clusters are notable by their rapid propagation. These systems might be expected to be the most rain-efficient producers because of their well-defined and organized mesoscale up- and downdrafts. Houze et al. (1990) also found that springtime major rain events in Oklahoma are associated with rapidly moving squall lines. Applying a mean speed criterion to refine a preselection based on cloud extension at 213 K is thus a logical step. The mean speed calculation is based on the mean displacement of the cloud geometric center between initiation and dissipation of the 213-K cluster. Similar to Fig. 2, Fig. 3 presents the number fraction and cloud coverage fraction at 233 K as a function of the mean speed at 213 K. One-third of the MCSs retained in the first step (6% of the total population of MCSs) have a mean speed below 10 m s^{-1}, and two-thirds (12% of the total population of MCSs) have a mean speed larger than 10 m s^{-1}. The coverage fraction decreases slightly (from 87% to 78%) when the mean speed increases from 0 to 10 m s^{-1}. The speed threshold of 10 m s^{-1} was thus retained to eliminate slow-moving MCSs that are associated with a moderate 233-K cloud coverage. In summary, the new stratification procedure proposed here is as follows:

1) In a population of MCSs defined at the 233-K threshold, only those containing at least one 213-K cluster lasting for 3 h or more are kept. They represent 18% in number and 87% in 233-K cloud coverage.
2) In a second step, the selected systems without any 213-K clusters moving faster than 10 m s^{-1} are discarded.

The selected systems are called organized convective systems (OCSs). They account for 78% of the total 233-K cloud cover while representing only 12% of the total MCSs number. Based on the above-mentioned papers of Houze (1981) and Houze et al. (1990), there are good reasons to assume that the fast-moving large MCSs are the organized systems such as squall lines. Even though it is not possible with the data available to us to confirm this inference rigorously, the label ''organized'' seems appropriate for the classification proposed here.

c. Cloud-cover climatological description of MCSs, OCSs, and MCCs in the Sahel

The cloud-cover climatological description of the Sahelian MCSs has been studied in detail by Mathon and Laurent (2001). This section compares some statistics of the MCC and OCS subpopulations with those computed for the whole MCS population. MCCs are identified using the Maddox criteria adapted to our temperature thresholds by linear extrapolation:

1) area >80 000 km^2 at the 233-K threshold,
2) area >30 000 km^2 at the 213-K threshold,
3) criteria 1 and 2 during at least six consecutive hours, and

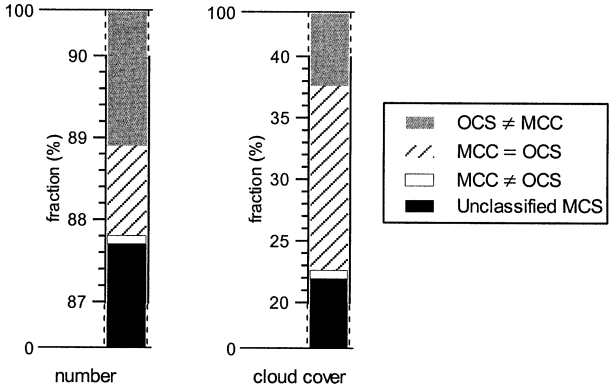

FIG. 4. Contribution of OCSs, MCCs, and unclassified MCSs in term of (left) number and (right) 233-K cloud cover.

4) eccentricity (minor axis/major axis) >0.7 at time of maximum extent at 233-K threshold.

There are, on average, 1947 MCSs, 217 OCSs, and 23 MCCs per year over the Sahel. MCC and OCS contributions to the total MCS number and cloud cover are presented in Fig. 4. As already mentioned, OCSs account for 78% of the 233-K cloud cover and represent 12% of the total MCS number. In comparison, MCCs represent 16% of the cloud cover and 1.2% of the MCS number. As one might suspect, MCC and OCS subsets overlap. Indeed only 8% of the MCC population do not satisfy the OCS criteria. Figure 5 shows the mean annual number (Fig. 5a) and cloud cover (Fig. 5b) of OCSs, MCCs, and MCSs versus their life span for 2-h classes. Every long-lived MCS (lifetime longer than 24 h) is classified as OCS, which means that all long-lived MCC also satisfy OCS criteria.

The above MCC statistics confirm that MCCs represent a too-small share of the cloud cover in the perspective of a comprehensive climatological study. A similar result will be found below (see section 5) regarding rainfall. Note that, in their study carried out over the whole of Africa with 3-h temporal-resolution Meteosat images, Laing and Fritsch (1993) identified 195 MCCs in 2 yr. They show a map on which about 60 MCCs are positioned over the Sahel, which is an average of 30 per year. Given the fact that they worked at a warmer threshold (240 K) and over the whole year, this statistic compares well with our figure of 23 MCCs per year, which applies to the core of the rainy season only.

The spatial distributions of OCS and MCC cover are summarized in Fig. 6 as their contributions to the total MCS coverage. The two populations have a similar spatial distribution with a maximum contribution between approximately 10° and 15°N. This figure shows clearly that the central Sahel is a privileged location for large organized convection extending from 11°–12°N to 15°–16°N and from 10°W to 15°E. This is related to the presence of a midlevel jet (the African easterly jet) that provides a vertical wind shear favoring the development of large convective systems, such as squall lines (e.g., Lafore and Moncrieff 1989). To the south of 10°N, MCCs explain less than 10% of the MCS coverage, and the share of OCSs drops down to less than 40%.

The mean annual spatial distribution of OCS and MCC occurrences at initiation and dissipation time are plotted in Fig. 7. Only OCSs and MCCs that cross the

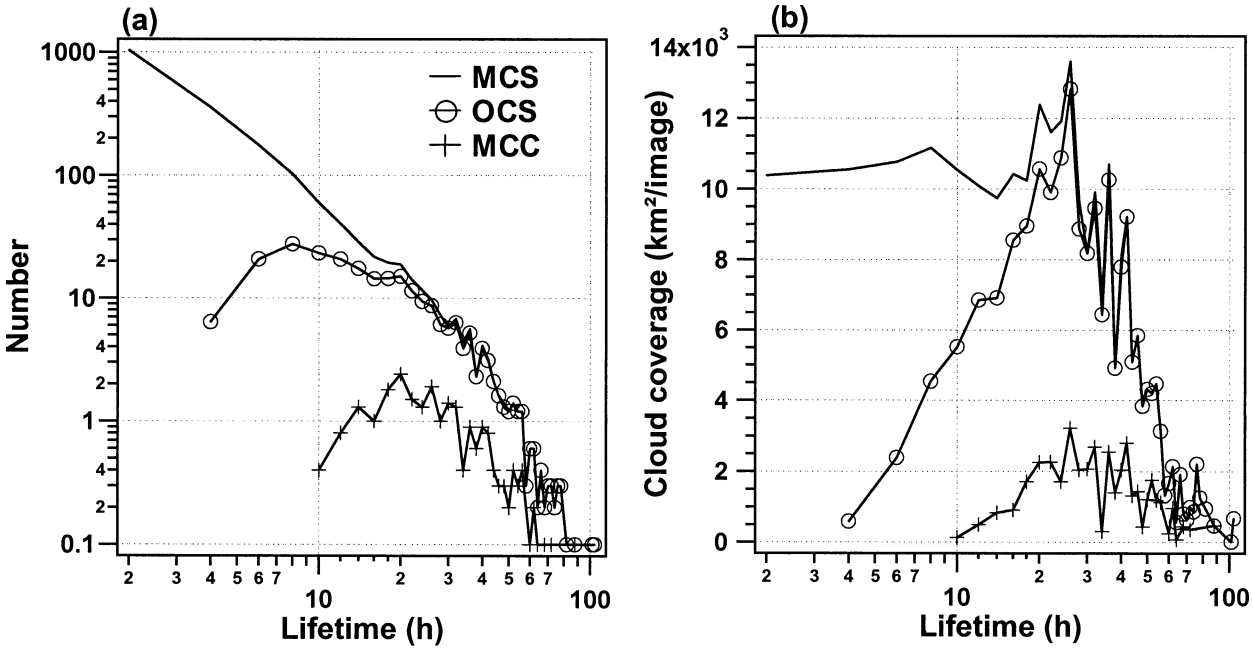

FIG. 5. Mean annual distributions of MCS, OCS, and MCC (a) number and (b) 233-K cloud cover (square kilometers per image) vs lifetime. Results were obtained over the central Sahel area during nine summers.

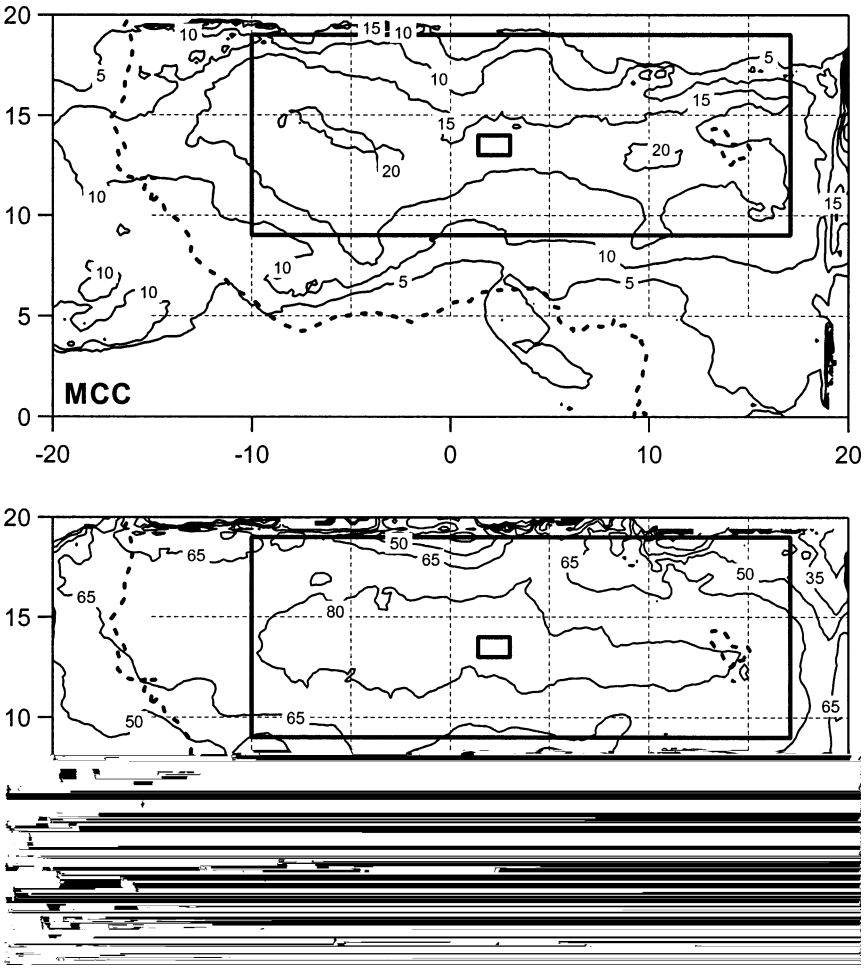

FIG. 6. Spatial distributions of MCC and OCS contribution (%) to the total MCS cloud coverage. Results were obtained over nine summers at a threshold of 233 K. The central Sahel area and the EN area are enclosed. The dashed contours delineate the continent.

central Sahel area, delineated as the large boldface rectangle, are taken into account. Most of the OCSs or MCCs that cross the central Sahel are initiated within the area itself. Some of them are initiated to the east of the area; the maximum observed on the right-hand side of the map is an artifact corresponding to the edge of the satellite images used.

Although the MCC initiation map does not display any clear preferential location of initiation, the effect of orography appears clearly when looking at OCS initiation. For instance, the Jos Plateau (9°N, 8°E) and the Air massif (18°N, 8°E) are places of maximum generation occurrence. Both MCC and OCS dissipations are shifted westward and southward in relation to their initiations. Dissipation can occur far to the west of the Sahel zone (as far as 30°W). Most of OCS dissipations occur in the 10°–15°N belt and about one-half of the MCC population dissipates outside of the Sahel area.

5. Rainfall climatological description of the Sahelian MCSs

To evaluate the rainfall characteristics of the satellite-observed MCSs, it was necessary to build a population of events comparable to that defined from rainfall data as defined in section 3b. This consisted of selecting MCSs according to their overlapping surface with the EN area. Both the temperature threshold and the overlapping surface threshold were investigated so as to explain most of the major rain events (see section 3c) while eliminating most of the other cases. The best compromise was obtained when 80% of the EN area is covered by a cluster at a threshold of 233 K. Note that this overlapping ratio is very similar in magnitude to the ground-based criterion used to select major rain events.

The MCSs that are potentially important in terms of rainfall over the EN study area are defined at 233 K as follows:

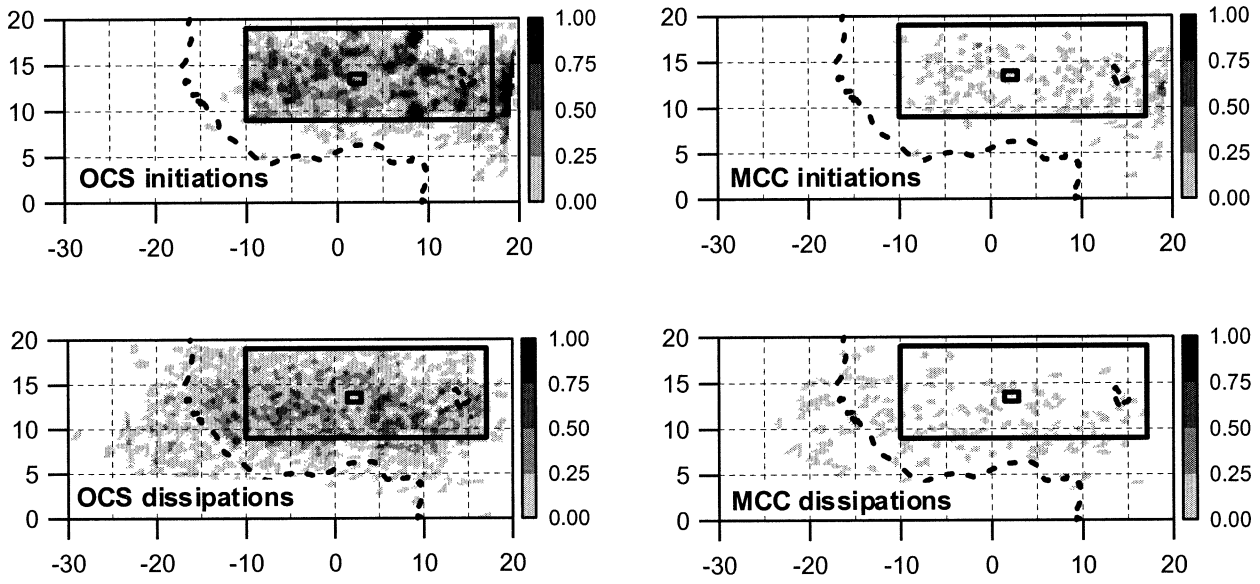

FIG. 7. Mean annual occurrences of MCCs and OCSs at initiation time and dissipation time. Only MCCs or OCSs that have crossed the central Sahel area have been taken into account. Results were obtained over nine summers at 233 K. Boxes and dashed contours are the same as in Fig. 6.

1) t0 is the time at which the MCS first covers at least 1 pixel belonging to the study area,
2) the event ends at t1, which is when the system has totally left the EN area, and
3) between t0 and t1, there must be at least one image in which 80% of the EN area is covered by the system.

Most of these events are associated with a single MCS. However, in 25% of the cases several MCSs are involved. This may be a problem for an objective estimation of the contribution of each MCS type. A calculation based on interpolated rainfall data (with comparable time–space resolution between satellite and rainfall information) indicates that in such cases 83% of rainfall can be attributed to the leading MCS. Thus, one can reasonably and objectively associate a rain event, as defined in section 3b, to a single MCS.

a. Total rainfall

Over the 9 yr of this study, and for the period 1 July–15 September, a total of 530 MCSs covered at least 25 km^2 of the EN study area (i.e., 1 pixel in Meteosat images) at any moment of their life cycle. However, only 186 of these 530 MCSs satisfy the criterion for overlapping as defined above. Referring to these events as ''EN MCSs,'' it is calculated that, on average, 21 of them are observed each year, producing 301 mm (83% of the total rainfall observed on the ground).

TABLE 4. Annual statistics of the EN convective systems for 1 Jul–15 Sep.

	Total	EN MCS	EN OCS	EN MCC
Number		21	19	3
Cumulative rainfall (mm)	361	301 (83%)	280 (78%)	57 (16%)

OCS and MCC contributions to the total rainfall have been investigated. It is seen in Table 4 that there are, on average, 19 EN OCSs per year, against 3 EN MCCs per year (EN OCSs and EN MCCs refer to the subpopulations of the EN MCSs satisfying, respectively, the OCS and MCC criteria). The subpopulations of EN OCSs and EN MCCs represent roughly 10% of the corresponding total populations of Sahelian systems: over the 9 yr of our study, 171 EN OCSs were recorded, as compared with 1949 OCSs over the whole Sahel (9%), and 26 EN MCCs, as compared with 211 MCCs over the whole Sahel (12%). The OCSs produce 280 mm (78% of the total rainfall observed on the ground), that is, 14.7 mm per event, on average. The EN MCCs are more efficient because they produce 57 mm (16% of the total rainfall observed on the ground), that is, 19 mm per event. All the statistics given above are nonconditional area averages over the EN study area, that is, they integrate rainy and nonrainy areas. Again, they apply to the core of the rainy season—D'Amato and Lebel (1998) have shown that convective systems tend to be less rain efficient during the margins of the rainy season.

One can wonder to what extent the subpopulation of EN rain events defined from the gauge network matches the subpopulation of EN OCSs. In comparing the statistics of Table 2 with those of Table 4, it is seen that the EN rainfall share of the EN OCSs (78%) is in between the share of all of the EN rain events (91%) and that of the EN major rain events (73%). At the same time, the contingency statistics of Table 5 show that

TABLE 5. Contingency table of EN rain events vs EN convective systems. The MCS line corresponds to MCS for which at least 1 pixel overlapped the EN study area. EN MCS (EN OCS) is MCS (OCS) overlapping 80% of the EN study area during at least 0.5 h (one image).

	Isolated or no rain (a)	EN rain events (253 in total over the period of study) (b)	Major EN rain events (144 in total over the period of study)	Total (a) + (b)
MCS	277	253	144	530
EN MCS	14	172	136	186
EN OCS	0	171	134	171

there are more EN OCSs than EN major rain events. This deserves a few comments: (i) EN major rain events produce 16.5 mm of rain on average, whereas OCSs produce 14.7 mm on average; (ii) most *major* rain events (93% in number, accounting for 83% of the cumulative rainfall produced by the major events) are associated with an EN OCS; (iii) however, when considering *all* EN rain events, 100% of the EN OCSs are associated with an EN rain event; (iv) 92% of the EN MCSs are associated with an EN rain event (this accounts for 85% of the cumulative rainfall produced by the EN rain events). In addition, it was found that all of the EN MCCs are EN OCSs (it is only in the south of the Sahel that a few MCCs are not OCSs). The differences between the population of EN OCSs and the population of *major* rain events is linked to the 233-K cloud shield being larger than the precipitating area. Despite this, it is seen that the EN OCSs constitute a good proxy of the major rain events.

There is a last point to consider regarding the computation of these seasonal rainfall statistics. The raw computation of the OCS seasonal rainfall share certainly underestimates the real statistics. By considering only those convective systems that overlap more than 80% of the EN area, one eliminates small systems of little rain productivity but also eliminates OCSs with an unfavorable trajectory. Recall that such a selection procedure is needed to obtain a robust and objective method to be used in the absence of ground validation. When such a ground validation is available, as in the case here, one can systematically evaluate the marginal rain produced by the OCSs eliminated in the selection procedure. For instance, considering all the OCSs with at least 1 pixel overlapping the EN study area at any time of their life leads to the computation that an additional 15% of the seasonal rain is associated with the OCSs, increasing their total share to 93%. A realistic estimate of the total share of OCS rainfall during the core of the rainy season over the central Sahel thus may be around 90%.

b. Diurnal cycle

To characterize the diurnal cycle of a convective system, one would like to have an EN validation area ''traveling'' with the convective system. Here it is only possible to study the diurnal cycle of rainfall over a fixed area and relate it to the overpassage of convective systems at various stages of their life cycle. As seen from Fig. 8a, the diurnal cycle of the rain yield associated with the EN OCSs is very similar to the diurnal cycle of the total rainfall over the EN area. A large share of rainfall occurs between 0100 and 1000 LST. Such a feature is atypical because over land the convective activity is at a maximum during the evening rather than at night or early morning. It is obvious that the geo-

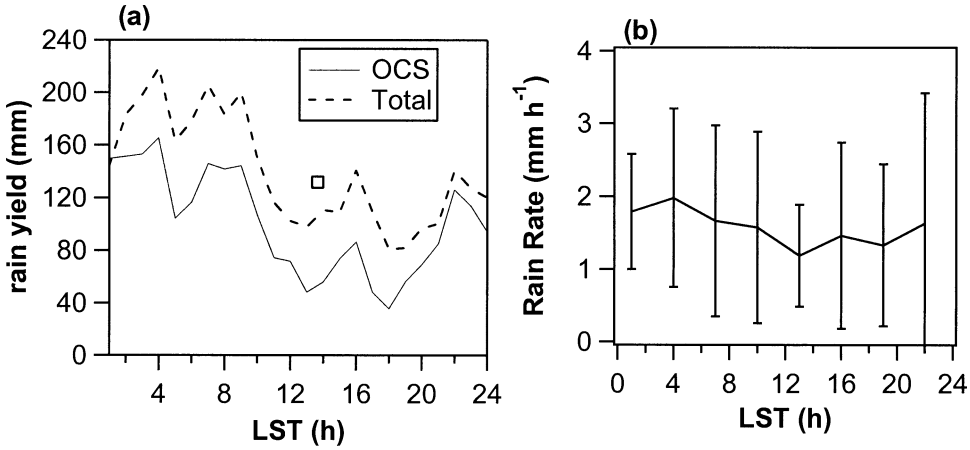

FIG. 8. (a) Diurnal variations of the total rain yield obtained from EN data (mm) and the rain yield associated with OCSs. (b) Averaged OCS mean rain rate vs mean time of first occurrence over the EN area. Associated standard deviations are also plotted. Results are obtained for nine summers.

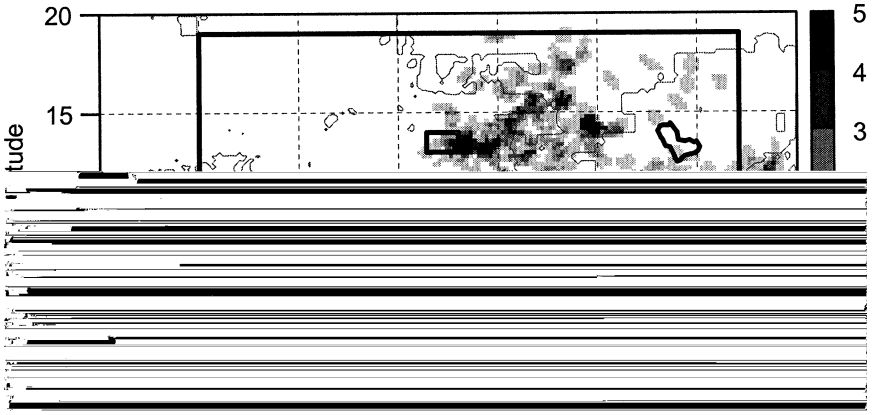

FIG. 9. Map of the mean annual number of initiations of the EN OCSs. The light contours indicate regions of elevation greater than 400 m. Indicated boxes are the same as in Fig. 6.

graphical location of the validation area must partly explain this result.

Figure 8b shows the mean rain rate of the EN OCSs versus the mean time of their occurrence over the EN area. The mean rain rate is calculated by dividing the rain yield of an event by its duration. It is seen that the OCSs tend to be slightly more rain efficient when they reach the EN area during nighttime. However, as indicated by standard deviations, there is a large scattering around the mean values. Thus, no clear modulation explaining the atypical diurnal cycle of Fig. 8a can be identified. This leads us to conclude that the nocturnal/early morning predominance of rainfall over the EN area is primarily due to the fact that OCSs occur more frequently over the study area during the night, because of their propagative nature, as already suggested by Shinoda et al. (1999). To check this finding, the location of generation of the EN OCSs is plotted in Fig. 9 along with the areas with an elevation above 400 m. Most of the events come from regions far from the EN area, and most of the initiations occur in areas above 400 m in altitude. The distances separating the validation area from the initiations are generally greater than 250 km. Because OCS initiations occur mostly in the afternoon over the Sahel (Mathon and Laurent 2001) and because the OCSs propagate mainly westward at 10–15 m s^{-1}, the probability of observing nocturnal occurrences over the EN area is enhanced. These results demonstrate that, in the EN area, the diurnal cycle of rainfall is significantly influenced by the orography located to the east.

6. Interannual variability

As shown by Le Barbé and Lebel (1997) at the regional and decadal scales, there is a relationship between the number of rain events (derived from daily rain gauge readings) and the corresponding rain yield in the Sahel. In the current paper, the use of two sources of data led to the definition of two populations of events with respect to the EN window of observation: (i) EN convective systems, observed from Meteosat, have a subpopulation of more efficient systems, the EN OCSs; and (ii) EN rain events, observed from the EN rain gauges, have a subpopulation of more efficient systems, referred to as the EN major rain events (see section 3c).

The question addressed here is whether the conclusions of Le Barbé and Lebel (1997) hold when looking at the interannual variability and whether the number of convective systems and the number of rain events display the same kind of relationship with the seasonal rainfall. Figure 10a shows that there is indeed a significant cofluctuation between the total rain yield over the period considered and the number of major events observed during that period, whether these events are satellite-defined (EN OCSs) or ground-defined (EN major rain events). Note that 1996 was the only year with more major rain events than OCSs. Note also that 1998 and 1999 are two untypical years (at least as can be ascertained from our limited sample of 9 yr); relative to the seasonal rainfall there are fewer EN rain events than expected in 1998, and in 1999 there are more EN OCSs than expected. One peculiarity of 1999 is that, while the number of EN major rain events is normal, the number of all the EN ground events is above normal (not shown), meaning that in this year an unexpectedly large number of smaller ground events were observed. This also means that the mean rain yield per event was smaller in 1999 and that a larger frequency of deep convective cloud occurrences may not correspond to a larger rain yield. Note that 1999 was the most cloudy year (threshold of 233 K, not shown) over the central Sahel during the last 10 yr and that, as a consequence, satellite rainfall estimates based on the counting of deep convective clouds occurrences [e.g., the global precipitation index method; Arkin (1979)] would predict a large seasonal total. According to the validation provided by the EN network, the rainfall would have been largely overestimated over the central Sahel that year.

It is clear that the good cofluctuation between the total seasonal rainfall and the number of events implies

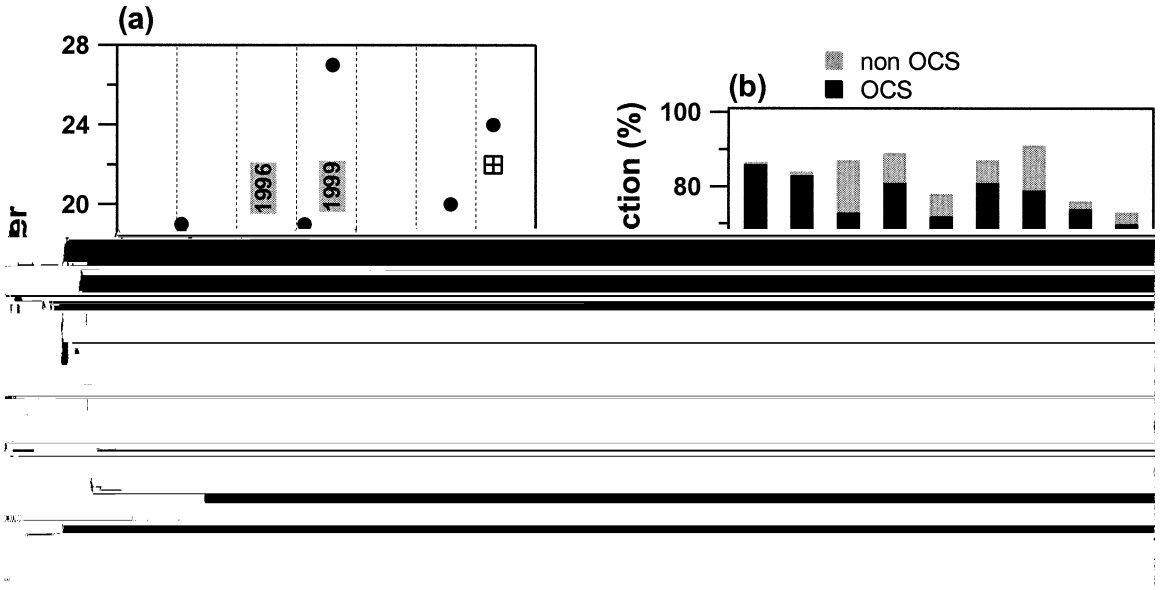

FIG. 10. (a) Number of EN major rain events and number of EN OCSs vs total rain yield between the 1 Jul and 15 Sep. (b) Contribution of the EN MCSs to the seasonal rain yield (the respective contributions of the EN OCSs and of the non-OCSs are shown).

that the fraction of total rain produced by these events is somewhat stable. This is confirmed by Fig. 10b, with the proportion of rain produced by the EN OCSs varying from 70% to 85%. It is striking that the years with the lowest share of OCS rainfall are the wet years: 1994, 1998, and 1999. Only in 1992, a moderately dry year, do we observe a similarly low share of the EN OCS rainfall. Despite some variability from year to year, it is well established from Fig. 10 that the number of OCSs is a good indicator of the abundance of the rainy season, always producing more than 70% of the total rain yield (and even more if one considers the correction applied to the seasonal statistics of the OCS rainfall at the end of section 5a). Keeping in mind the spatial distribution of the OCSs shown in Fig. 6, it can be concluded that the OCSs constitute a key element for understanding the interannual variability of rainfall over the Sahel.

7. Conclusions

The work presented here has two main objectives. One is to obtain reliable statistics for the rainfall produced by mesoscale convective systems over the Sahel, depending on their extension and degree of organization. The other is to identify the factors influencing the variability of these statistics. To reach these goals, two high-resolution datasets were used: full-resolution infrared images collected by Meteosat that cover the whole of the Sahel and direct rainfalls recorded by the dense EPSAT-Niger network of digitized rain gauges covering a 16 000-km^2 area in the region of Niamey. Both datasets span a common period of 9 yr, thus allowing for the computation of reliable statistics regarding the core of the rainy season (1 July–15 September).

For the period considered, it has been found that 90% of the total rainfall over the 16 000-km^2 EN area is produced by a small population of organized convective systems characterized by a 213-K cluster lasting for 3 h or more and moving at a speed of more than 10 m s^{-1}. This population of OCSs represents only 12% of the total population of MCSs—defined as 5000-km^2 cloud clusters at 233 K. The OCSs are also responsible for about 78% of the cloud cover at 233 K, which is a confirmation that, statistically, the 233-K cloud cover is a good proxy of ground rainfall. The average rain production of one OCS is 14.7 mm. This amount is less than the average rain produced by an MCC (defined from Maddox criteria), which is 19 mm. Hence, MCCs are more rain efficient than OCSs, but their frequency is much smaller (on average, 3 MCCs vs 19 OCSs are recorded during one rainy season over the 16 000-km^2 area) and they account for only 16% of the seasonal rainfall over the central Sahel.

Over the EN validation area, the comparison between the population of convective systems and the population of rain events shows that all of the OCSs are associated with a rain event identified from the rain gauge network. In fact, the share of the seasonal rainfall was computed to be 91% for the so-called EN rain events and was estimated to be around 90% for the OCSs. It is thus possible to build a coherent climatologic description of rain events based on the identification of OCSs from infrared imagery. To summarize, OCSs are large and fast-moving systems—this, as found in previous studies, implies some degree of organization—that account for most of the rain over the Sahel during the core of the rainy season.

The variability of the rainfall produced by MCSs is

determined by two factors: (i) their rate of occurrence and (ii) their intensity. In this paper, it has been shown that the interannual variability of rainfall in the region is mostly determined by the year-to-year fluctuation of the number of OCSs, which confirms results obtained previously from ground measurements (see e.g., D'Amato and Lebel 1998).

Beyond the initial goals of the study, the demonstration that it is possible to associate a single cloud system to a rain event at the mesoscale has important consequences for rainfall studies over a limited region. For instance, the hypothesis of Shinoda et al. (1999) on the origin of the nocturnal and early-morning peak of precipitation observed over the region of Niamey was confirmed. This is due to the propagative nature of the OCSs associated with orography-driven generations located a few hundred kilometers to the east of the validation area. Another application of this study is in the area of satellite rainfall estimation. It is known that a simple counting of cloud cover at 233 K may provide good rainfall estimates when a sufficiently large averaging is carried out in space and time. This may be related to our result showing that 233-K cloud cover is correlated well with the number of OCSs, which is itself correlated well with rainfall. At the same time, there is a random and significant variability of the average rain rate from one OCS to another. Algorithms that combine a satellite-based identification and tracking of the OCSs with a few ground measurements to enable an estimation of their average rain rate should, therefore, produce more robust rain estimates than a simple counting of the number of 233-K pixels.

Acknowledgments. We are grateful to Direction de la Météorologie du Niger, and especially to its director, Dr. A. Also, for our close collaboration in the operation of the EPSAT-Niger network. Special thanks are given to three anonymous reviewers for detailed comments and suggestions on the paper and to Nick Hall for helping to put it in proper English. This research was funded by IRD.

REFERENCES

Arkin, P. A., 1979: The relationship between fractional coverage of high cloud and rainfall accumulations during GATE over the B-scale array. *Mon. Wea. Rev.*, **107,** 1382–1387.

D'Amato, N., and T. Lebel, 1998: On the characteristics of the rainfall events in the Sahel with a view to the analysis of climatic variability. *Int. J. Climatol.*, **18,** 955–974.

Desbois, M., T. Kayiranga, B. Gnamien, S. Guessous, and L. Picon, 1988: Characterization of some elements of the Sahelian climate and their interannual variations for July 1983, 1984 and 1985 from the analysis of Meteosat ISCCP data. *J. Climate*, **1,** 867–904.

Duvel, J. P., 1989: Convection over tropical Africa and the Atlantic Ocean during northern summer. Part I: Interannual and diurnal variations. *Mon. Wea. Rev.*, **117,** 2782–2799.

Hamilton, R. A., and J. W. Archbold, 1945: Meteorology of Nigeria and adjacent territories. *Quart. J. Roy. Meteor. Soc.*, **71,** 231–235.

Houze, R. A., 1977: Structure and dynamics of a tropical squall line system observed during GATE. *Mon. Wea. Rev.*, **105,** 1540–1567.

——, 1981: Structure of atmospheric precipitation systems: A global survey. *Radio Sci.*, **16,** 671–689.

——, 1993: *Cloud Dynamics*. Academic Press, 573 pp.

——, B. F. Smull, and P. Dodge, 1990: Mesoscale organization of springtime rainstorms in Oklahoma. *Mon. Wea. Rev.*, **118,** 613–654.

Jobard, I., and M. Desbois, 1992: Remote sensing of rainfall over tropical Africa using Meteosat infrared imagery: Sensitivity to time and space averaging. *Int. J. Remote Sens.*, **13–14,** 2683–2700.

Lafore, J.-P., and M. W. Moncrieff, 1989: A numerical investigation of organization and interaction of the convective and mesoscale region of a tropical squall line. *J. Atmos. Sci.*, **46,** 521–544.

Laing, A. G., and J. M. Fritsch, 1993: Mesoscale convective complexes in Africa. *Mon. Wea. Rev.*, **121,** 2254–2263.

——, ——, and A. J. Negri, 1999: Contribution of mesoscale convective complexes to rainfall in Sahelian Africa: Estimates from geostationary infrared and passive microwave data. *J. Appl. Meteor.*, **38,** 957–964.

Laurent, H., T. Lebel, and J. Polcher, 1997: Rainfall variability in Soudano-Sahelian Africa studied from raingauges, satellite and GCM. Preprints, *13th Conf. on Hydrology*, Long Beach, CA, Amer. Meteor. Soc., 17–20.

Le Barbé, L., and T. Lebel, 1997: Rainfall climatology of the HAPEX-Sahel region during the years 1950–1990. *J. Hydrol.*, **188–189,** 43–73.

Lebel, T., and A. Amani, 1999: Rainfall estimation in the Sahel: What is the ground truth? *J. Appl. Meteor.*, **38,** 555–568.

——, H. Sauvageot, M. Hoepffner, M. Desbois, B. Guillot, and P. Hubert, 1992: Rainfall estimation in the Sahel: The EPSAT-Niger experiment. *Hydrol. Sci. J.*, **37,** 201–215.

——, J. D. Taupin, and N. D'Amato, 1997: Rainfall monitoring during HAPEX-Sahel: 1. General rainfall conditions and climatology. *J. Hydrol.*, **188–189,** 74–96.

Machado, L. A. T., M. Desbois, and J.-P. Duvel, 1992: Structural characteristics of deep convective systems over tropical Africa and the Atlantic Ocean. *Mon. Wea. Rev.*, **120,** 392–406.

——, W. B. Rossow, R. L. Guedes, and A. W. Walker, 1998: Life cycle variations of mesoscale convective systems over the Americas. *Mon. Wea. Rev.*, **126,** 1630–1654.

Maddox, R. A., 1980: Mesoscale convective complexes. *Bull. Amer. Meteor. Soc.*, **61,** 1374–1387.

Mathon, V., and H. Laurent, 2001: Life cycle of the Sahelian mesoscale convective cloud systems. *Quart. J. Roy. Meteor. Soc.*, **127,** 377–406.

Miller, D., and J. M. Fritsch, 1991: Mesoscale convective complexes in the western Pacific region. *Mon. Wea. Rev.*, **119,** 2978–2992.

Redelsperger, J.-L., and J.-P. Lafore, 1988: A three-dimensional simulation of a tropical squall line: Convection, organization and thermodynamic vertical transport. *J. Atmos. Sci.*, **45,** 1334–1356.

Roux, F., 1988: The West African squall line observed on 23 June 1981 during COPT 81: Kinematics and thermodynamics of the convective region. *J. Atmos. Sci.*, **45,** 406–426.

Rowell, D. P., and J. R. Milford, 1993: On the generation of African squall lines. *J. Climate*, **6,** 1181–1193.

Shinoda, M., T. Okatani, and M. Saloum, 1999: Diurnal variations of rainfall over Niger in the West African Sahel: A comparison between wet and drought years. *Int. J. Climatol.*, **19,** 81–94.

Smull, B. F., and R. A. Houze, 1985: A midlatitude squall line with a trailing region of stratiform rain: Radar and satellite observations. *Mon. Wea. Rev.*, **113,** 117–133.

Williams, M., and R. A. Houze, 1987: Satellite-observed characteristics of winter monsoon cloud clusters. *Mon. Wea. Rev.*, **115,** 505–519.

Zipser, E. J., 1977: Mesoscale and convective-scale downdrafts as distinct components of squall-line structure. *Mon. Wea. Rev.*, **105,** 1568–1589.